



Continuous packed bed adsorption of phenol and cyanide onto modified rice husk: an experimental and modeling study

Neetu Singh*, Chandrajit Balomajumder

Department of Chemical Engineering, Indian Institute of Technology, Roorkee, India, Tel. +91 8869038022; emails: neeturbs@gmail.com (N. Singh), chandfch@iitr.ernet.in (C. Balomajumder)

Received 21 September 2015; Accepted 21 December 2015

ABSTRACT

The current study estimates the feasibility of modified rice husk (MRH) in eliminating phenol and cyanide from binary aqueous solution through packed bed column studies. The influence of varying initial concentration, flow rate, and bed depth on the performance of packed column was examined. The experimental data for the packed bed column were applied in different kinetic model such as the Thomas, Adams–Bohart, Yoon–Nelson, and Wolborska model to calculate the breakthrough curve and to define the representative parameters of the packed bed column beneficial for scheming large-scale column studies. The Thomas model is to be found best for phenol, whereas Yoon–Nelson Model provided good agreement with experimental data ($R^2 > 0.85$) for both phenol and cyanide. This model was designed to calculate the 50% breakthrough time attained by the packed bed column system and provided the predictable breakthrough time for the packed bed columns that were not exhausted throughout the process. Average relative error was applied to estimate the characteristics of the predicted and experimental values under the corresponding models to observe the best fit model. The MRH packed bed column could be effectively used up to six cycles of adsorption/desorption for the elimination of phenol and cyanide, respectively.

Keywords: Breakthrough study; Cyanide; Dynamic modeling; Modified rice husk; Phenol; Packed bed column

1. Introduction

In current years, there has been significant attention in the treatment of wastewater produced by industrial processes. Coke wastewater produced from the coke process of steel plant contains several toxic compounds with high concentrations [1,2]. Phenol and cyanide comprising wastewater may not be accompanied into surface water without prior treatment because of the poisonous nature of pollutants. Phenol,

cyanide, and their compounds are among the utmost universal pollutants and they are extensively well known to be toxic. The maximum contaminant limit (MCL) in industrial release has been set at 0.5 mg/L for phenol and 0.2 mg/L for cyanide by World Health Organization (WHO), central pollution control board (CPCB), and US environmental protection agency (USEPA) [3]. Low concentrations of phenol contact can cause eyes and skin harms, nuisance, vomiting, central nervous system, lung, liver, kidney, and heart harm, eventually foremost to death. On the other hand, cyanide can cause coma, heart pains, inhalation

*Corresponding author.

sicknesses, headaches, and even death [4,5]. Different skills have been established and are accessible to eliminate phenol and cyanide from industrial effluent, avoiding the contamination of the environment.

Adsorption using granular-activated carbon (GAC) in different reactor arrangements has been the most used technologies for the treatment of industrial wastewater comprising phenol and cyanide pollutants. The continuous removal process of pollutants has increased pronounced attention in current years [6,7]. A number of research have been carried out on the treatment of phenol and cyanide comprising wastewater by using fluidized bed reactors, biofilm reactors, rotating biological contactor reactor, and membrane-based reactors [5–10]. Use of such treatment techniques requires high cost and constant contribution of chemicals, which converts unrealistic and uneconomical. Hence, effective, low cost and sustainable techniques are mandatory for treatment of wastewater. Usually, adsorbents offer a large surface area to interact with pollutants [11,12,14,15]. The adsorption process by GAC is established to be the best accessible technology for the removal of pollutants from wastewater [3,11,12]. But due to high cost and regeneration problem, reduce the industrial use of GAC for the adsorption process.

The exploration of easily available and a low-cost adsorbent has led to the search of biological and agricultural source of biomass, as adsorbents. Various investigators have been motivated on the use of cheap substitute adsorbents comprising natural materials, biosorbents, and waste byproducts from agriculture and industry source for pollutants removal from wastewater [11–18]. The adsorption process by using different types of agricultural source biomass has increased reliability in current years because of its outstanding performance and simplicity of strategy for treatment of wastewater [11,12].

The modified rice husk (MRH), is profuse agromonic low cost products, is able of eliminating phenol and cyanide and can be measured as an effective adsorbent for treatment of phenol and cyanide. In current years, consideration has been taken on the application of modified or unmodified rice husk as an adsorbent for the elimination of phenol and cyanide [13–17]. Continuous flow of pollutant results achieving equilibrium and adsorbent regeneration is to be necessary after this phase. Owing to this feature, breakthrough study becomes necessary for calculation of performance and design of the packed bed [19,20].

In this paper, the adsorption features of phenol and cyanide on MRH synthesized in the laboratory was studied in laboratory-scale packed bed column with variable parameters of the inlet flow rate of pollutants, initial concentration, and bed depth. The

performance and breakthrough curve features of the MRH for the simultaneous removal of phenol and cyanide from binary aqueous solution via continuous packed bed column were also evaluated. Continuous column dynamics have been carried out by Adams–Bohart model, Thomas model, Wolborska model, and Yoon–Nelson model.

2. Materials and methods

2.1. Reagents

Phenol and cyanide were obtained from Himedia Laboratories Pvt. Ltd. Mumbai, India. All analytical reagents (AR) grade chemicals were used in this study.

2.2. Instrumentation

The concentrations of phenol and cyanide were determined by colorimetric picric acid and 4-aminoantipyrine methods, respectively, by UV–vis spectrophotometer [18]. The Brunauer–Emmett–Teller (BET) surface area of MRH was calculated by using a surface area analyzer (ASAP 2010 Micrometrics, USA). The pH of solutions was measured by standard methods using pH meter provided by WTW[®] Germany (makes pH 720). The SEM images of loaded and unloaded adsorbents were collected by using a scanning electron microscope (LEO 435 VP). The bulk density of adsorbent was determined by using a MAC bulk density meter. In packed bed experiments, a peristaltic pump (PP- 20) procured from Miclins India, Chennai was used to feed the phenol and cyanide solution through-out the packed bed.

2.3. Preparation of adsorbate

Adsorbate solutions were prepared by dissolving appropriate quantity of phenol and cyanide in millipore water. The concentration of 500 mg/L for phenol and 50 mg/L for cyanide was used for packed bed column study.

2.4. Preparation and characterization of adsorbent

2.4.1. Preparation and characterization MRH

Rice husk collected from a local market in Roorkee, India, was used in this experiment. Rice husk was washed with millipore water for three times in order to take away dirt and other contaminations. Then the adsorbent materials were dried in an oven under the temperature of 60°C for 24 h. The rice husk was

modified by using 2 N H₂SO₄ solution at a ratio of 1:2 solid to liquid for 24 h to increase pore volume and surface area. After that, MRH was washed with millipore water until the complete acid removes and dried at 60°C to completely remove moisture and stored in an air tight vessel for further use. Spectral analysis using Fourier Transform Infrared (FTIR, Nicolet 6700, USA) was used to define the functional groups existing onto the surface of the MRH before and after adsorption.

2.5. Continuous packed bed adsorption study

Continuous packed bed adsorption experiments were accompanied using a column of 3 cm diameter and 93.1 cm height. A runs of experiments were carried out to study the influence of packed bed height (18, 36, 54, 72, and 93.1 cm), feed flow rate (440, 220, and 146.6 mL/h), and initial phenol and cyanide concentration in ratio (100:10, 300:30, and 500:50 mg/L). The experiments were conducted by the varying flow rate of the solution using initial concentrations of 500 mg/L for phenol and 50 mg/L for cyanide. Solution with known concentration of phenol and cyanide was pumped from the bottom of the packed bed column at a varying flow rate of 440 mL/h using a peristaltic pump (Fig. 1). The treated samples at the outlet of the packed bed column were obtained at fixed time intervals. Subsequently packed column

exhaustion the phenol and cyanide loaded adsorbent was regenerated with 0.1 N HCl by using flow rate 440 mL/h. Thereafter, adsorbent bed was washed with millipore water two times and the regenerated bed was reprocessed in additional cycle.

2.5.1. Calculation of breakthrough curve parameters

The performance of the continuous packed column was estimated by breakthrough curve. The breakthrough curves demonstrate the packing performance of phenol and cyanide to be eliminated from solution in a packed bed [19]. Generally, the breakthrough curve was defined by normalized concentration as C_f/C_i , in which C_f and C_i signify the final and initial concentration of pollutants, respectively. The curve was expressed as normalized concentrations against the contact time or effluent volume:

$$V_{\text{eff}} = Q \cdot t_{\text{total}} \tag{1}$$

where V_{eff} is the volume of effluent (L), Q is the volumetric flow rate (mL/h), and t_{total} represent total flow time (h).

The total adsorbed phenol and cyanide amount (q_{total} (mg)) at saturation in the continuous packed column for a given initial concentration and flow rate is obtained from:

$$q_{\text{total}} = \frac{Q \cdot A}{1000} = \frac{Q}{1000} \int_{t=0}^{t=t_{\text{total}}} C_{\text{ad}} \cdot dt \tag{2}$$

where Q and A are the flow rate (mL/h) and the area under the breakthrough curve, respectively.

The total amount of phenol and cyanide, sent to packed column (M_{total}) is designed from Eq. (3):

$$M_{\text{total}} = C_i \cdot Q \cdot t_{\text{total}}/1000 \tag{3}$$

Total percentage removal of phenol and cyanide (performance of packed bed column) can be calculated from the equation given below:

$$\text{Total percentage removal} = \frac{(C_i - C_f)}{C_i} \times 100 \tag{4}$$

Equilibrium uptake (exp) of phenol and cyanide (maximum capacity of the packed bed column) can be defined by Eq. (5) as the total amount of phenol and cyanide adsorbed (q_{total}) per unit of dry weight of adsorbent (M) in the column:

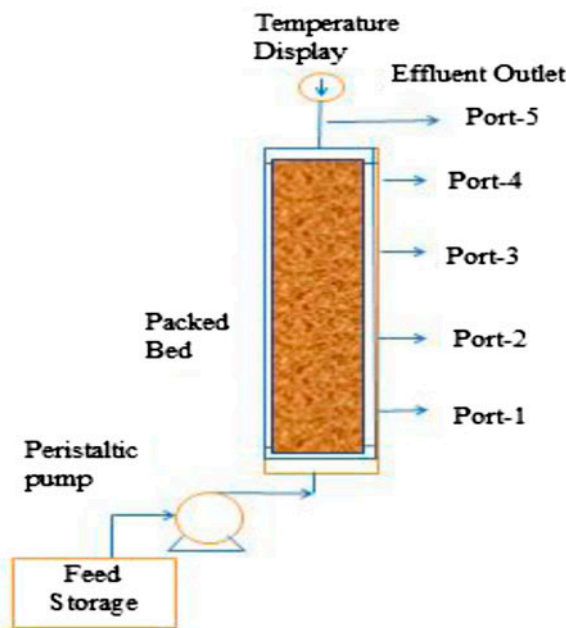


Fig. 1. Schematic diagram of continuous packed bed column.

$$Q_{e(\text{exp})} = \frac{q_{\text{total}}}{M} \quad (5)$$

The influence of packed column adsorption height is determined through mass transfer zone (MTZ) [20].

To determine the length of MTZ from breakthrough curve following expression given below:

$$\text{Mtz } H_{\text{tz}} = H \frac{t_{\text{ex}} - t_{\text{b}}}{t_{\text{ex}}} \quad (6)$$

where H_{tz} is the height of the MTZ, H is the bed depth (cm), t_{b} is the time required to reach breakthrough point(hour), and t_{ex} is the time required to reach exhaustion (h).

2.6. Packed bed modeling study

The nature of breakthrough curve and breakthrough time are considerable features in determining the dynamic behavior of an adsorption packed bed column [19,20]. The breakthrough curve defines the performance of the packed bed column. Various mathematical models have been established to analyze the breakthrough curve for phenol and cyanide adsorption in packed columns.

2.6.1. Adams–Bohart model

In general, Adams–Bohart model or bed depth service time model is one of the simplest and extensively used model for describing adsorption in packed bed column [20]. This model was established on the approximation of parameters characteristics as kinetic constant and adsorption capacity. The model is established on the surface reaction theory. Adams–Bohart model provide a widespread methodology for estimating column dynamics.

Non linear form of the Adams–Bohart model is expressed by equation given below:

$$\ln(C_f/C_i) = K_{\text{AB}} C_i t - K_{\text{AB}} N_0 (H/U_0) \quad (7)$$

where C_i and C_f are the influent and effluent concentrations (mg/L), respectively, K_{AB} is the Adam–Bohart kinetic constant (L/mg/h), N_0 is the adsorption capacity (mg/L), H is the height of the adsorbent bed (cm), t is time (h), and U_0 is the linear velocity (cm/h) calculated from the ratio of volumetric flow rate to the bed section area.

2.6.2. Thomas model

The Thomas model has been used to explain the breakthrough of a packed column and the describing adsorption parameters of the packed column [21,22]. This model was described that the rate driving force obeys the second-order law of reversible reaction kinetics. This model follows Langmuir kinetics and the constant separation factor. No axial dispersion at minimum bed height and the breakthrough happened instantly after the flow started [23].

The Thomas model is stated in a non-linearized form, as shown in given equation:

$$C_f/C_i = 1/1 + \exp\left(K_{\text{th}} q_{\text{m}} \frac{M}{F} - K_{\text{th}} \times t\right) \quad (8)$$

where C_i and C_f are the influent and effluent concentrations (mg/L), respectively, K_{th} is the Thomas rate constant (mL/mg/h), q_{m} is the maximum adsorption capacity (mg/g), M is the mass of adsorbent in column (g), and F is the influent flow (mL/h).

2.6.3. Wolborska model

The Wolborska model was focused on the estimation of parameter kinetic coefficients of the external mass transfer (h^{-1}) [24,25]:

$$C_f/C_i = \exp\left(\frac{\beta_a C_i t}{N_0} - \frac{\beta_a H}{U_0}\right) \quad (9)$$

where β_a is kinetic coefficient of the external mass transfer (h^{-1}).

The parameter β_a is defined by equation:

$$\beta_a = \frac{U_0}{2D} \left(\sqrt{1 + \frac{4\beta_a D}{U_0^2}} - 1 \right) \quad (10)$$

where C_i and C_f are the influent and effluent concentrations (mg/L), respectively, β_a reflects external mass transfer coefficient with a negligible axial dispersion coefficient (D). Negligible axial dispersion occurs at low bed height or feed flow rate is very high through the column. β_a reflects the influence of both axial dispersion and mass transfer in liquid phase. The Wolborska model will equivalent to the Adams–Bohart model if parameter $\beta_a/N_0 = K_{\text{AB}}$.

2.6.4. Yoon–Nelson model

This model was based on the statement that the rate of reduction in possibility of adsorption for individually adsorbate is proportional to the possibility of adsorbate breakthrough on the adsorbent and the possibility of adsorbate adsorption [26,27]. This model is not as much of complex than other models and needs less or no full data regarding the features of the adsorbate, the physical properties of adsorbent packed in the bed, and the type of adsorbent [27].

The Yoon–Nelson model expression is given by the equation:

$$\frac{C_f}{C_i} = \frac{\exp(k_{YN}t - \tau k_{YN})}{1 + \exp(k_{YN}t - \tau k_{YN})} \quad (11)$$

where C_i and C_f are the influent and effluent concentrations (mg/L), respectively, k_{YN} is rate constant (h^{-1}), t is time (h), and τ is the time required for 50% adsorbate breakthrough (h).

2.6.5. Error analysis

To evaluate the best appropriate model from the best fit to the experimental data, it is essential to study the experimental data by error analysis. Error analysis approaches such as the average relative error (ARE), have been used in the present study to obtain the model which is better fitted to the experimental values [28].

The differences between experimental data and data acquired from above-mention model can be analyzed by given error function:

$$\text{ARE} = \frac{1}{n} \sum_{i=1}^n \left| \frac{(C_f/C_i)_{\text{cal}} - (C_f/C_i)_{\text{exp}}}{(C_f/C_i)_{\text{exp}}} \right| \quad (12)$$

where superscript cal and exp indicate the calculate data from models and experimental data, and n is the number of measurements.

3. Results and discussions

3.1. Characterization of adsorbents

The moisture content, ash content, and fixed carbon for MRH before adsorption were found 8.81, 23.3, and 32.6, respectively. The bulk density of adsorbent was determined by using a MAC bulk density meter, which was found to be 130.6 kg/m^3 . The surface area and pore volume of MRH were found $410 \text{ m}^2/\text{g}$ and $1.90 \times 10^{-2} \text{ cc/g}$.

Fig. 2 represents the morphology of SEM image of rice husk: (a) for raw rice husk (RRH), (b) for MRH before adsorption, and (c) for MRH after adsorption as seen by scanning electron microscopy (SEM). The spongy structure and plane morphology of MRH makes it appropriate adsorbent as it improves the adsorption ability. The surface morphology of MRH is changed from being plane to uneven. The occupation of pores designates adsorption of phenol and cyanide in the pores and surface of MRH providing it an uneven surface.

The chemical nature of adsorbent and functional group presents on adsorbents were estimated by using FTIR, Nicolet Avatar 370 CsI spectrometer (Thermo Electron Corporation, USA). Fig. 3 represents the FTIR spectrum of MRH before and after adsorption. It is evident from figure that functional groups amine, carbonyl, carboxylic acid, alkyl, and C–N were present on the surface of adsorbent. FTIR vibrations available on the surface of MRH before the adsorption of phenol and cyanide, i.e. $3,300\text{--}3,500$, $2,500\text{--}3,100$, $2,850\text{--}2,960$, $1,540\text{--}1,870$, $1,030\text{--}1,230$, cm^{-1} displaced weak and reduced reflectance pattern between $3,300$ and $3,500$, corresponds to vibrations of –OH and –NH functional group and $2,500\text{--}3,100$ corresponds to vibrations of –CH groups [29]. It could be noticed that the maximum of the peaks was decreased after loading of phenol and cyanide on the surface of MRH, indicating the adsorption onto the surface of MRH. An absorption group equivalent to Si–O extends at $1,033.30 \text{ cm}^{-1}$ governs and the band at wave number $800\text{--}850 \text{ cm}^{-1}$ corresponding to Si–C stretching was established. From figure, it could be detected that adsorption of phenol and cyanide onto MRH observed from reduced in the peaks of functional groups around $1,030\text{--}1,230 \text{ cm}^{-1}$, $1,540\text{--}1,870 \text{ cm}^{-1}$, $3,300\text{--}3,500 \text{ cm}^{-1}$, and $2,850\text{--}2,960 \text{ cm}^{-1}$. The occurrence of phosphate groups and Si–OH groups on the MRH surface are liable for adsorption. Consequently, it can be established that MRH existing a satisfactory surface morphology for adsorption of phenol and cyanide.

3.2. Effect of experimental parameters on breakthrough curve

3.2.1. Influence of bed depth

The breakthrough curve acquired for adsorption of phenol and cyanide on MRH for five different bed depth 18, 36, 54, 72, and 93.1 cm at a fixed flow rate 440 mL/h and inlet flow concentration 500 mg/L for phenol and 50 mg/L for cyanide given in Fig. 4. With decrease in bed depth, axial dispersion occurrences led in the mass transfer and abridged the diffusion of

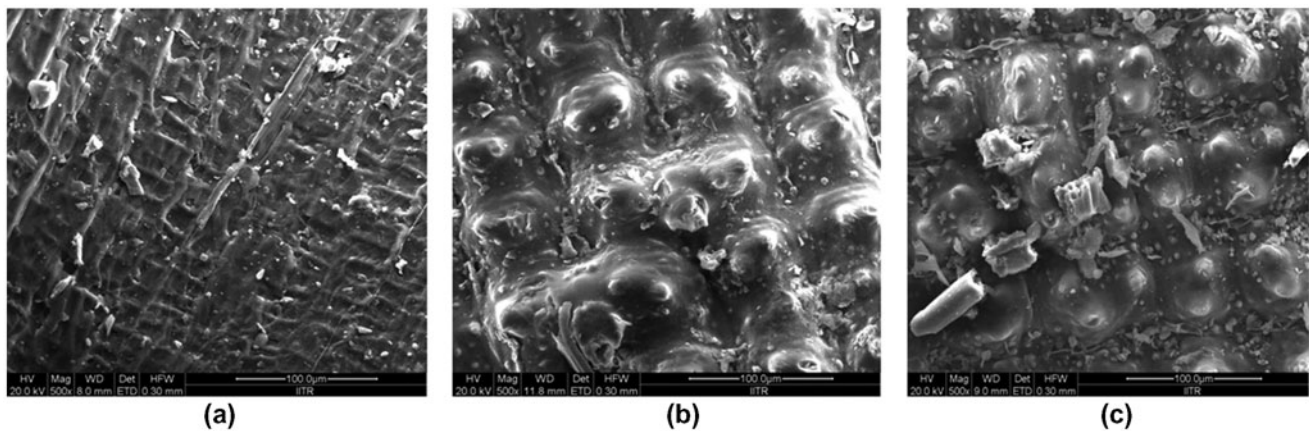


Fig. 2. SEM image of rice husk: (a) for RRH, (b) for MRH before adsorption, and (c) for MRH after adsorption.

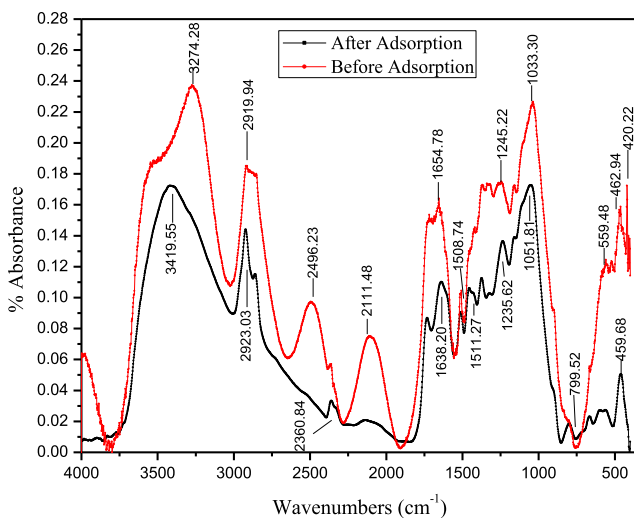


Fig. 3. FTIR spectrum of MRH before and after adsorption.

phenol and cyanide. The adsorbate did not have enough time to disperse into the entire of the adsorbent [30]. The MTZ increase with bed depth and moves in a continuous column from the inlet of the packed bed and keep on near the outlet. Therefore, for constant influent concentration and bed system, high bed depth would produce a lengthier interval from the MTZ to reach at the exit of packed column afterward resulting a lengthy breakthrough time. With decreased bed height, the breakthrough for both phenol and cyanide followed quickly and the bed column exhausted faster. The height of packed bed strongly affected the column breakthrough time. The $Q_{e(\text{exp})}$ of phenol for different bed depth 18, 36, 54, 72, 93.1 cm, were 1,341.46, 1,038.68, 794.65, 670.24, 610.59 mg/g, respectively, and the $Q_{e(\text{exp})}$ of cyanide were 83.91, 77.61, 70.47, 85.96, 81.54 mg/g, respectively.

3.2.2. Influence of flow rate

The influence of flow rate on the adsorption of phenol and cyanide on MRH was observed by changing the feed flow rate (440, 220 and 146.6 mL/h) with adsorbent bed height of 93.1 cm and initial concentration 500 mg/L of phenol and 50 mg/L of cyanide. Breakthrough curves for the adsorption of phenol and cyanide by MRH continuous packed column to varying flow rate given in Fig. 5. It is demonstrated from figure that at higher flow rate, the column was saturated quickly as a result the breakthrough time decreased for both phenol and cyanide [31]. At the lowest flow rate 146.6 mL/h, the breakthrough curves for both phenol and cyanide were detected to have a slow but sure curve than 220 and 440 mL/h. The maximum adsorption capacity of the packed column increased with increased flow rate for both phenol and cyanide (Table 1). At high flow rate, the interaction time between adsorbate and adsorbent were comparatively short. Therefore, the adsorption was not widespread and resulted in a sharp breakthrough curve [32–34]. The $Q_{e(\text{exp})}$ of phenol for different flow rate 440, 220, and 146.6 mL/h, were 610.59, 384.80, 243.39 mg/g, respectively, and the $Q_{e(\text{exp})}$ of cyanide were 81.54, 48.24, 33.22 mg/g, respectively.

3.2.3. Influence of initial concentration of adsorbate

Packed bed adsorption experiments were accompanied with variable influent concentrations of phenol and cyanide. Fig. 6 illustrates the influence of the inlet concentration of adsorbate solution ranging from 100, 300, 500 mg/L for phenol and 10, 30, 50 mg/L for cyanide at a constant flow rate 440 mL/h, of MRH packed bed height 93.1 cm. It can be observed that an increase in the initial phenol and cyanide

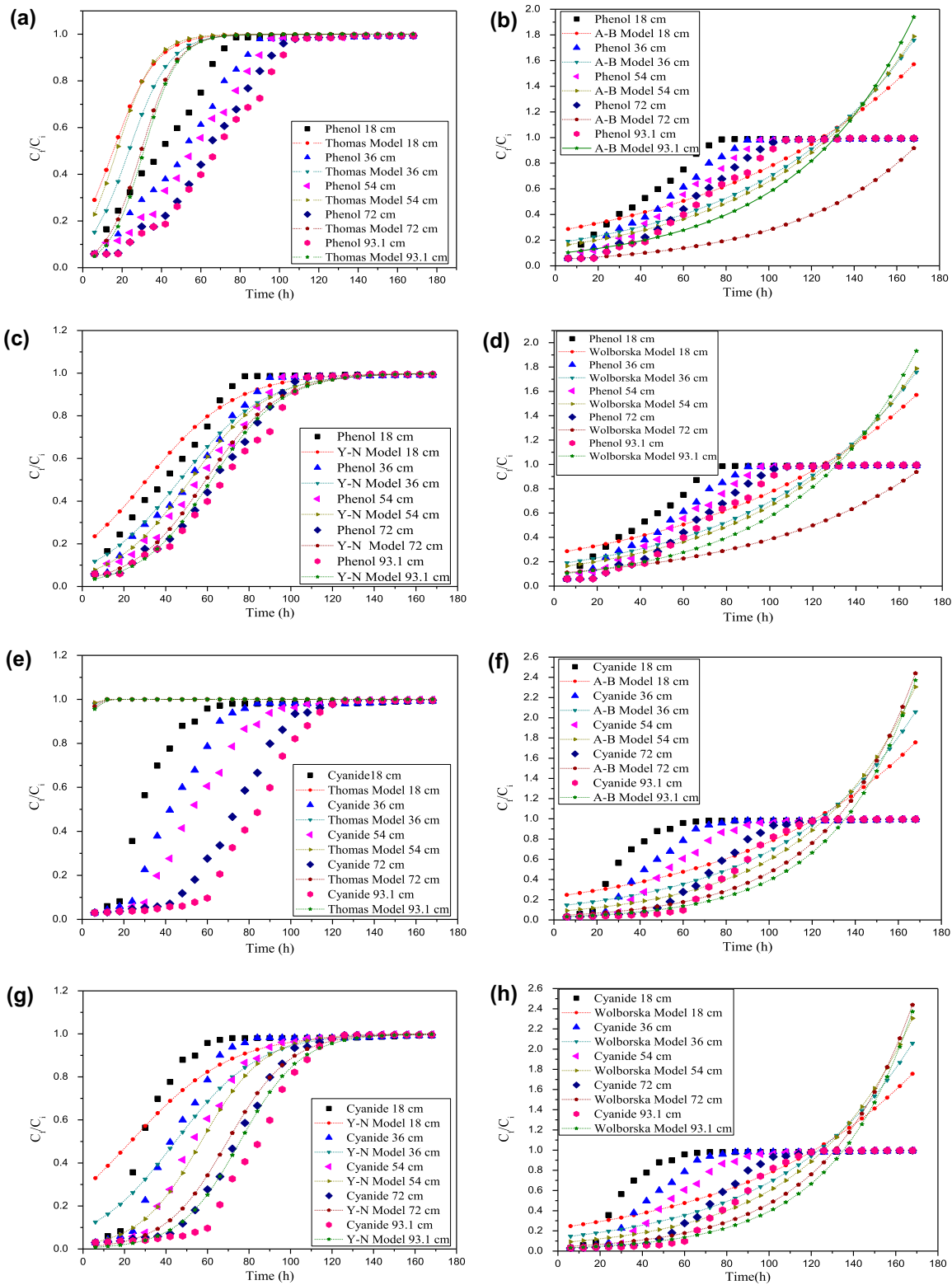


Fig. 4. Effect of bed depth: (a) phenol removal predicted by the Thomas model, (b) phenol removal predicted by the Adam-Bohart model, (c) phenol removal predicted by the Yoon-Nelson model (d) Phenol removal predicted by the Wolborska model, (e) cyanide removal predicted by the Thomas model, (f) cyanide removal predicted by the Adam-Bohart model, (g) cyanide removal predicted by the Yoon-Nelson model, and (h) cyanide removal predicted by the Wolborska model.

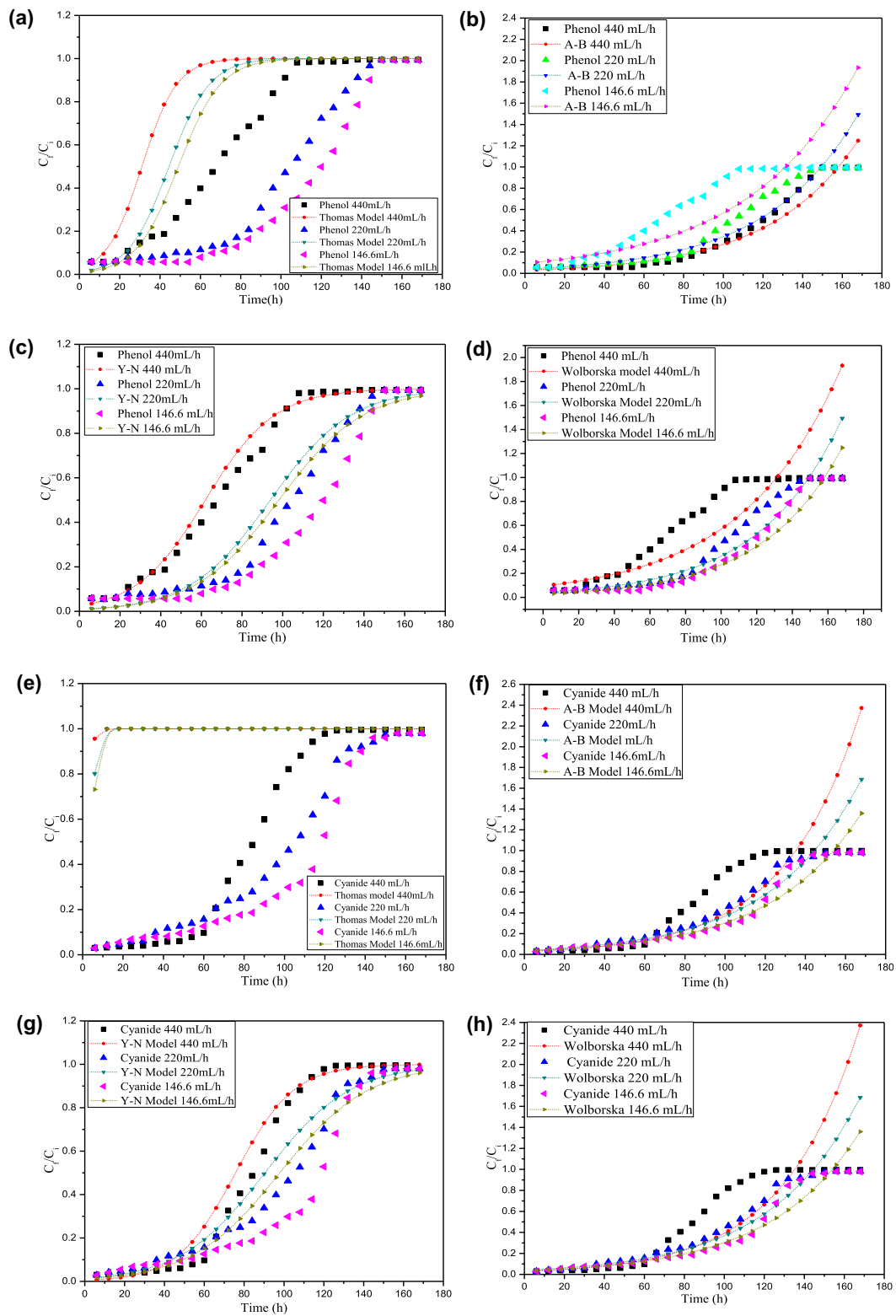


Fig. 5. Effect of flow rate: (a) phenol removal predicted by the Thomas model, (b) phenol removal predicted by the Adam-Bohart model, (c) phenol removal predicted by the Yoon-Nelson model, (d) phenol removal predicted by the Wolborska model, (e) cyanide removal predicted by the Thomas model, (f) cyanide removal predicted by the Adam-Bohart model, (g) cyanide removal predicted by the Yoon-Nelson model, and (h) cyanide removal predicted by the Wolborska model.

Table 1
Mathematical description of continuous packed bed column parameters

Adsorbate	Q (mL/h)	M (g)	C _i (mg/L)	H (cm)	q _{total} (mg)	M _{total} (mg)	Total removal (%)	Q _{e(exp)} (mg/g)	V _{eff} (L)
Phenol	440	1,250	500	93.1	7632.33	14,520	52.56	610.59	29,040
	220	1,250	500	93.1	4809.99	12,540	38.36	384.80	25,080
	146.6	1,250	500	93.1	3042.35	9,682.20	31.42	243.39	19,360.40
	440	246	500	18	3,300	13,200	25.00	1341.46	26,400
	440	492	500	36	5,110.29	13,200	38.71	1038.68	26,400
	440	738	500	54	5864.57	13,200	44.42	794.65	26,400
	440	984	500	72	6595.19	14,520	45.42	670.24	29,040
	440	1,250	500	93.1	7632.33	14,520	52.56	610.59	29,040
	440	1,250	100	93.1	3177.01	4,224	75.21	254.16	42,240
	440	1,250	300	93.1	6115.37	9,504	64.35	489.23	31,680
	440	1,250	500	93.1	7632.33	14,520	52.56	610.59	29,040
Cyanide	440	1,250	50	93.1	1019.3	1,716	59.40	81.54	34,320
	220	1,250	50	93.1	602.96	1,122	53.74	48.24	22,440
	146.6	1,250	50	93.1	415.21	880.02	47.18	33.22	17600.40
	440	246	50	18	206.42	924	22.34	83.91	18,480
	440	492	50	36	381.82	1,188	32.14	77.61	23,760
	440	738	50	54	520.08	1,320	39.40	70.47	26,400
	440	984	50	72	845.86	1,584	53.40	85.96	31,680
	440	1,250	50	93.1	1019.30	1,716	59.40	81.54	34,320
	440	1,250	10	93.1	332.97	475.2	70.07	26.64	47,520
	440	1,250	30	93.1	805.52	1,267.20	63.57	64.44	42,240
	440	1,250	50	93.1	1,019.30	1,716	59.4	81.54	34,320

concentrations decreases the volume treated earlier to saturation of the packed bed, as shown in Table 1. At high adsorbate concentrations, the adsorbent bed was saturated more quickly thus declining the breakthrough curve and decrease the breakpoint time with increase in initial concentration [33]. The $Q_{e(\text{exp})}$ of phenol for different initial concentration 100, 300, 500 mg/L, were 254.16, 489.23, 610.59 mg/g, respectively, and the $Q_{e(\text{exp})}$ of cyanide for initial concentration 10, 30, 50 mg/L were 26.64, 64.44, 81.54 mg/g, respectively.

An extended breakthrough curve was obtained at the decrease in the initial concentration of phenol and cyanide demonstrating that more solution could be passed through the packed bed. This is owing to the circumstance that poorer concentration gradient produced a leisurelier conveyance as a result reduction in mass transfer coefficient [19,35].

3.3. Modeling of packed bed column

3.3.1. Thomas model

The experimental data were fitted to Thomas model for prediction of the breakthrough results. The Thomas kinetic constant (K_{th}) and a maximum

capacity of adsorption (Q_0) obtained from the slope and intercepts of linear plots of $\ln[(C_i/C_f) - 1]$ against t [36]. To obtain the best fit, the statistical error functions ARE was calculated. The model and breakthrough curves relating to bed depth, flow rate, and initial phenol and cyanide concentrations are presented in Figs. 4, 5 and 6. The values of Thomas model parameters for phenol and cyanide are listed in Tables 2 and 3, respectively. It is evident from table that Thomas rate constant and adsorption capacity increase with flow rate. However, the increase initial concentration of phenol, decreased the value of Thomas rate constant and increased the value of packed bed capacity Q_0 . This situation can be recognized to the more driving force due to the more amounts of phenol and cyanide passed through the packed bed [37,38]. The value of packed bed capacity Q_0 decreased and the K_{th} Thomas rate constant increased with increased bed depth. Comparable tendency has been detected by Aksu and Gönen [39]. For cyanide columns, the value of K_{th} and Q_0 of the Thomas model has similar trend as phenol data (Table 3). The R^2 values also indicated that the Thomas model fitted better for the phenol than the cyanide (Table 3). The maximum uptake capacity from Thomas model was found to be 1,090.80 mg/g for

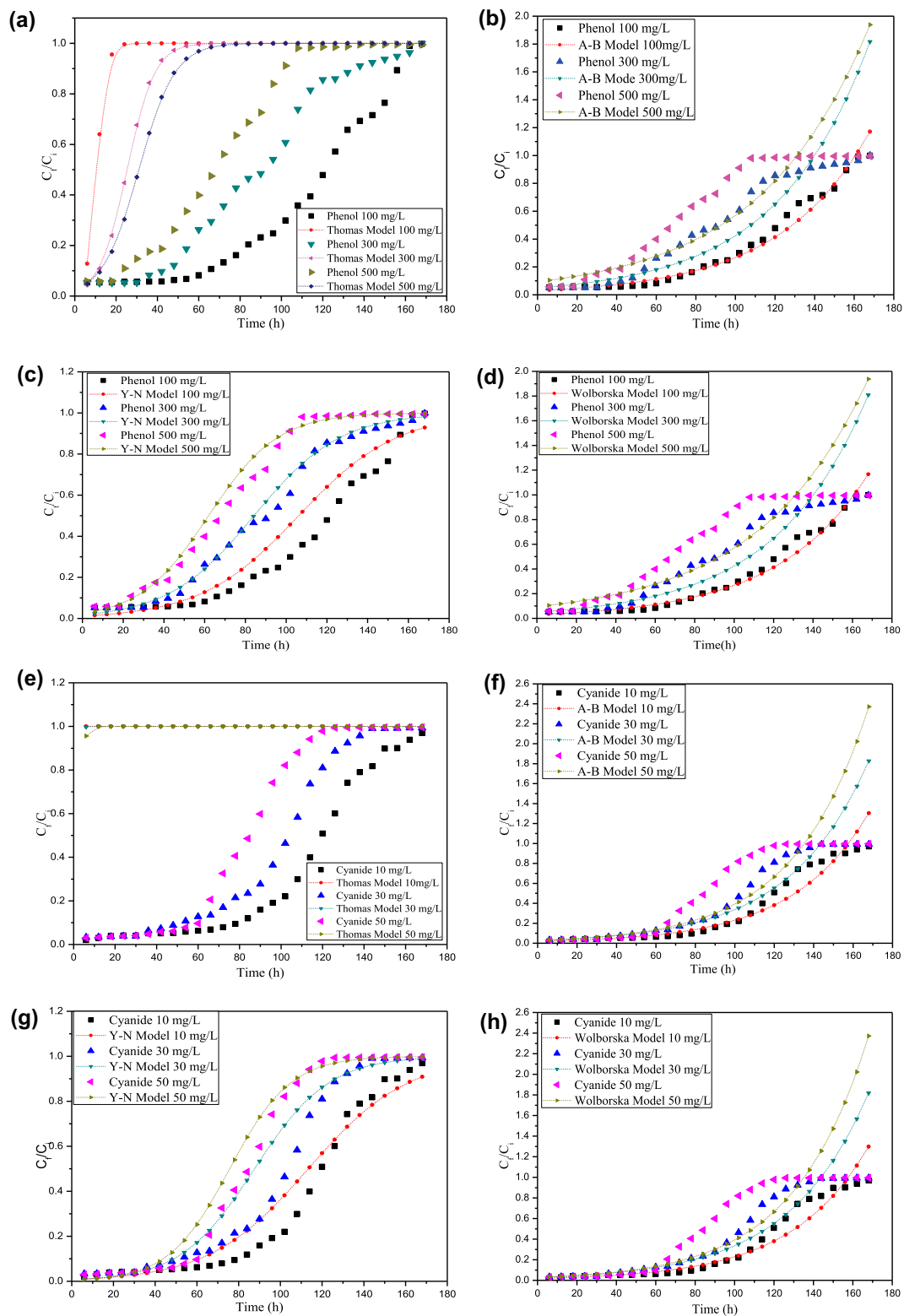


Fig. 6. Effect of initial concentration: (a) phenol removal predicted by the Thomas model, (b) phenol removal predicted by the Adam–Bohart model, (c) phenol removal predicted by the Yoon–Nelson model, (d) phenol removal predicted by the Wolborska model, (e) cyanide removal predicted by the Thomas model, (f) cyanide removal predicted by the Adam–Bohart model, (g) Cyanide removal predicted by the Yoon–Nelson model, and (h) Cyanide removal predicted by the Wolborska model.

Table 2

Parameters evaluated by the Thomas and Adams–Bohart model at different flow rates, bed depth, and the initial concentrations of phenol

Q (mL/h)	C_i (mg/L)	Kth (mL/h mg)	H (cm)	Q_0 (mg/g)	R^2	ARE	U_0 (cm/min)	k_{AB} (L/mg min)	N_0 (mg/L)	R^2	ARE	
440	1,250	500	0.0012	93.1	1,090.80	0.97	0.15	8,753.50	0.000036	6175557.64	0.82	0.17
220	1,250	500	0.0010	93.1	782.38	0.87	0.44	4,376.80	0.000043	3513044.95	0.96	0.05
146.6	1,250	500	0.0010	93.1	575.87	0.82	0.74	2,918.50	0.000045	2478592.21	0.95	0.07
440	246	500	0.0009	18	2,771.00	0.85	0.09	8,753.50	0.000021	30389465.74	0.58	0.12
440	492	500	0.0010	36	2,097.60	0.92	0.12	8,753.50	0.000027	15414466.24	0.68	0.18
440	738	500	0.0011	54	1,546.50	0.95	0.17	8,753.50	0.000029	10412011.46	0.75	0.16
440	984	500	0.0012	72	1,328.60	0.97	0.16	8,753.50	0.000035	10515315.55	0.79	2.61
440	1,250	500	0.0012	93.1	1,090.80	0.97	0.17	8,753.50	0.000036	6175557.64	0.82	0.17
440	1,250	100	0.0042	93.1	373.68	0.81	0.51	8,753.50	0.000217	1512658.23	0.97	0.50
440	1,250	300	0.0016	93.1	891.56	0.93	0.30	8,753.50	0.000071	3955833.76	0.90	0.12
440	1,250	500	0.0012	93.1	1,090.80	0.97	0.17	8,753.50	0.000036	6175557.64	0.82	0.17

Table 3

Parameters evaluated by the Thomas and Adams–Bohart model at different flow rates, bed depth, and initial concentrations of cyanide

Q (mL/h)	C_i (mg/L)	Kth (mL/h mg)	H (cm)	Q_0 (mg/g)	R^2	ARE	U_0 (cm/min)	k_{AB} (L/mg min)	N_0 (mg/L)	R^2	ARE	
440	1,250	50	0.0139	93.1	133.20	0.95	0.39	8,753.50	0.0005	636603.66	0.89	0.30
220	1,250	50	0.0094	93.1	79.55	0.96	0.44	4,376.80	0.0004	340132.58	0.96	0.04
146.6	1,250	50	0.0091	93.1	57.43	0.89	0.51	2,918.50	0.0004	241585.38	0.98	0.02
440	246	50	0.0083	18	206.14	0.73	0.12	8,753.50	0.0002	2953803.86	0.42	0.40
440	492	50	0.0101	36	199.15	0.84	0.18	8,753.50	0.0003	1503967.06	0.57	0.49
440	738	50	0.0134	54	170.90	0.98	0.24	8,753.50	0.0004	1021526.77	0.68	0.53
440	984	50	0.0135	72	155.79	0.97	0.34	8,753.50	0.0005	798251.50	0.83	0.37
440	1,250	50	0.0139	93.1	133.20	0.95	0.39	8,753.50	0.0005	636603.60	0.88	0.30
440	1,250	10	0.0422	93.1	39.91	0.93	0.57	8,753.50	0.0026	148377.10	0.97	0.53
440	1,250	30	0.0189	93.1	92.87	0.93	0.46	8,753.50	0.0008	406013.10	0.96	0.06
440	1,250	50	0.0139	93.1	133.2	0.95	0.39	8,753.50	0.0005	636603.60	0.88	0.30

phenol and 133.20 mg/g for cyanide at bed depth 93.1 cm and feed flow rate of 440 mL/h. Chowdhury et al. [40] obtained maximum uptake capacity was 7,257.32 mg/g for manganese (II). Woumfo et al. [41] obtained maximum capacity was 1,751.21 mg/g for phosphate in continuous packed bed column.

3.3.2. The Adams–Bohart model

The Adams–Bohart model was used for explanation of the first part of breakthrough curve. This methodology concentrated on the approximation of parameters including adsorption capacity N_0 and the mass transfer coefficient K_{AB} . In this study, linear plot of $\ln(C_f - C_i)$ against time t , at varying flow rates, bed depth, and initial concentration of phenol and cyanide were plotted. Slope and intercept of the curve were used to evaluate mass transfer coefficient K_{AB} and

saturation concentration N_0 , respectively. The experimental and calculated breakthrough curves regarding bed depth, flow rate, and initial phenol and cyanide concentrations are revealed in Figs. 4, 5, and 6. The values of K_{AB} and N_0 and other statistical error parameter for phenol and cyanide are summarized in Tables 2 and 3, respectively. It is apparent from the Table 2 that mass transfer coefficient K_{AB} increased with increase in bed depth and reduced with increased initial concentration and flow rate, whereas the value of N_0 increased with increased initial concentration and flow rate and reduced with increased bed height for phenol column. In the case of cyanide, the values of N_0 and K_{AB} of the Adams–Bohart model have a minor difference between the phenol data. The mass transfer coefficient K_{AB} increased with flow rate and bed height and decreased with initial concentration. This designated that the kinetics of the system

were controlled by external mass transfer [19,42]. The value of N_0 is to be found increased with increased flow rate and initial concentration and reduced with increased bed depth for cyanide (Table 3). This is due to the fact that when the flow rate increased for both phenol and cyanide, the volume of adsorbate that arrived the packed bed column was higher and caused the packed bed to saturate prior with a higher load of phenol and cyanide. This situation is also realistic in the case for the increase in the initial concentration of pollutants, through which the adsorbent in the packed column attained comparative exhaustion as the pollutant loading, was more. It is also evident from Figs. 4, 5, and 6, that the Adams–Bohart model applied only the initial part of the breakthrough curves for both phenol and cyanide. These investigations demonstrate that the adsorption kinetics is subsidized by the physical mass transfer of the packed bed column system [33].

3.3.3. Yoon–Nelson model

The Yoon–Nelson model is applied in the present work to prediction the breakthrough accomplishments. Less column data are required for construction of the model values. The values of k_{YN} and τ were obtained from the slope and intercepts of the linear plots between $\ln[(C_f/(C_i - C_f))]$ against t at varying bed depths, flow rates, and initial concentrations predict the rate constant and time required for 50% adsorbate breakthrough. This model showed that the 50% breakthrough for phenol and cyanide in the bed height 93.1 cm were at 61.98 and 75.70 h, respectively (Tables 4 and 5). The values of k_{YN} were found to increase with increasing bed heights, flow rate, and initial concentrations for phenol. However, the values of τ decreases with increases in initial concentration and flow rate and increased with increasing bed height. A similar tendency was found for biosorption of hazardous dye and Cd (II) for continuous packed bed column [35,43]. In the packed columns, the value of model parameter k_{YN} and τ have a same trend in cyanide data (Table 5).

3.3.4. Wolborska model

The Wolborska model was representative for the explanation of the first portion of the breakthrough curve [20]. The values of β_a were obtained from the slope and intercepts of the linear plots between $\ln[(C_f/C_i)]$ vs. t at different bed heights, flow rates, and initial concentrations. The parameter of Wolborska model kinetic coefficient β_a of the external mass transfer was found to increase with increasing flow

rate and reduced with increasing bed height and initial concentration for both phenol and cyanide indicated in Tables 4 and 5, respectively. β_a is an effective coefficient, which replicates the influence of mass transfer in aqueous phase and axial dispersion. This model detected that at lesser bed depth or at high flow rates through the column, the axial diffusion is insignificant as a result, β_a is equivalent to β_o , the external mass transfer coefficient. With increasing flow rate, the value of β_a found increased, subsequently increased turbulence decreases the film boundary layer nearby the adsorbent particle [39]. Predicted and experimental breakthrough curves with respect to flow rate, bed height, and initial phenol and cyanide concentration are shown in Figs. 4, 5, and 6, respectively. It is clear from tables and figures that there is a better contract between the experimental and calculated values.

Essentially, the packed bed column behaviors can be evaluated and assumed for advance design consequences and enhancement works over the models realistic in this current study. The models used in this study were appropriate for adsorption. The Thomas model offers evidence about the mass transfer between the phenol and cyanide solution and the MRH, which designate the driving force under different parameters. The Adam–Bohart model is often used to calculate the adsorption capacity of the adsorbent. The data provided for this model can be used to supply evidence for a large-scale wastewater treatment system [44]. Though, this model requires extra parameters and calculation to obtain the modeling data. The model often defines the adsorption that happens with surface reaction, the available adsorption place, and the initial part of the breakthrough [45]. The benefit of applying the Yoon–Nelson model is that it provides the information about the 50% column breakthrough and the mathematical application is very direct, which permits the exhaustion period of the column to be forecast without a long period for experimental time. This model required the minimum parameters and theoretical data calculation. The models used in this study fitted well for confident column parameters, whereas some parameters were not well signified by the models this is due to fact that the mass transfer resistance occurred and also the joined removal mechanisms involved [45].

3.4. Regeneration capacity of MRH

For the adsorption process to be feasible, effectual regeneration of the MRH packed bed is essential. Reusability of an adsorbent can be determined by equating the adsorption presentation of regenerated

Table 4

Parameters evaluated by the Yoon–Nelson and Wolborska model at different flow rates, bed depth, and initial concentrations of phenol

Q (mL/h)	M (g)	H (cm)	C_i (mg/L)	k_{YN} (min ⁻¹)	τ (min)	R^2	ARE	β_a (h ⁻¹)	R^2	ARE
440	1,250	93.1	500	0.0594	61.98	0.97	0.03	222.08	0.82	0.17
220	1,250	93.1	500	0.0510	93.92	0.89	1.20	151.76	0.96	0.05
146.6	1,250	93.1	500	0.0488	98.16	0.82	1.30	111.04	0.95	0.07
440	246	18	500	0.0472	30.99	0.85	0.04	638.18	0.58	0.14
440	492	36	500	0.0493	46.89	0.92	0.03	422.35	0.68	0.18
440	738	54	500	0.0539	51.88	0.95	0.01	306.11	0.75	0.16
440	984	72	500	0.0576	59.32	0.97	0.01	276.03	0.79	0.79
440	1,250	93.1	500	0.0594	61.98	0.97	0.03	222.08	0.82	0.17
440	1,250	93.1	100	0.0416	106.16	0.81	0.46	327.89	0.97	0.04
440	1,250	93.1	300	0.0475	84.25	0.93	0.08	281.74	0.90	0.13
440	1,250	93.1	500	0.0594	61.98	0.97	0.03	222.08	0.82	0.17

Table 5

Parameters evaluated by the Yoon–Nelson and Wolborska model at different flow rates, bed depth, and initial concentrations of cyanide

Q (mL/h)	M (g)	H (cm)	C_i (mg/L)	k_{YN} (min ⁻¹)	τ (min)	R^2	ARE	β_a (h ⁻¹)	R^2	ARE
440	1,250	93	50	0.0694	75.70	0.95	0.49	337.39	0.88	0.30
220	1,250	93	50	0.0472	90.40	0.96	0.08	152.37	0.96	0.04
146.6	1,250	93	50	0.0453	97.88	0.89	0.23	106.78	0.98	0.02
440	246	18	50	0.0417	23.05	0.73	0.09	714.82	0.42	0.39
440	492	36	50	0.0505	44.53	0.84	0.08	490.29	0.57	0.49
440	738	54	50	0.0674	57.00	0.98	0.03	406.56	0.68	0.53
440	984	72	50	0.0680	69.68	0.97	0.10	387.95	0.83	0.37
440	1,250	93	50	0.0694	75.70	0.95	0.49	337.39	0.88	0.30
440	1,250	93	10	0.0422	113.40	0.93	0.23	379.43	0.97	0.05
440	1,250	93	30	0.0569	87.63	0.93	0.51	339.70	0.96	0.06
440	1,250	93	50	0.0694	75.70	0.95	0.49	337.39	0.88	0.30

Table 6

Performance of MRH packed bed column during six cycles of phenol and cyanide sorption and desorption

Cycles	Phenol		Cyanide	
	Sorption (mg/g)	Desorption (mg/g)	Sorption (mg/g)	Desorption (mg/g)
1	10.12	9.8	1.50	1.30
2	9.98	8.9	1.40	1.20
3	9.91	8.7	1.20	0.96
4	9.90	7.7	1.10	0.87
5	8.7	6.6	1.00	0.78
6	6.9	5.1	0.99	0.70

adsorbent with the original adsorbent. The column adsorption performance was carried out for six sorption/desorption cycles using 0.1 N HCl as an eluting agent through the packed bed in the upwards flow direction at a flow rate 440 mL/h for 2 h. MRH packed in column of 93.1 cm height and 500 mg/L of phenol and 50 mg/L of cyanide initial concentration

tested for sorption/desorption cycles. Percent desorption of adsorbed phenol and cyanide were approximately >85% after three cycles [46]. The amount of phenol and cyanide adsorbed by the packed column gradually decreased with the cycle progress (Table 6). The loss of regeneration capacity is owing to trouble in retrieving binding sites as the cycles progress [47].

4. Conclusions

The operation of the continuous packed bed reactor was investigated in this present work for the treatment of high strength wastewater, in order to estimate phenol and cyanide elimination capability. This study indicated that the MRH prepared from rice husk was promising for removing phenol and cyanide from wastewater in continuous packed bed reactor. FTIR and SEM have been applied to examine the characterization of MRH before and after adsorption. The elimination of phenol and cyanide from binary aqueous solution was conducted in a continuous packed bed column system with varying the bed height, flow rate, and initial concentration. The change in bed length significantly affected the packed bed column performance by slowing the exhaustion time and enhanced the column performance. The percentage removal of phenol and cyanide were significantly increased with the increase in bed height or adsorbent dosage. Though, the increases in initial concentration and flow rate of phenol and cyanide have a tendency to speed up the exhaustion of the packed bed column. Comparison of breakthrough curves acquired from modeling and experimental work demonstrated a very worthy agreement between them. Thomas, Adams–Bohart, Yoon–Nelson, and Wolborska models effectively predicted breakthrough curves attained under varying experimental conditions. Thomas and Yoon Nelson model indicated good agreement for phenol. The Yoon Nelson model valued the 50% breakthrough curve and provided the evaluation breakthrough time for packed bed column. The Adam–Bohart model evaluated the packed column and experimental data, which forecast the capacity of the packed bed column systems. Adams–Bohart and Wolborska models were fitted to the initial part of breakthrough curves of phenol and cyanide representing adsorption under numerous experimental conditions. The MRH adsorbent indicated good reusability throughout numerous adsorption/desorption cycles. The results from MRH bioassays were predominantly encouraging for the use of the continuous process as an efficient treatment technique high strength toxic wastewaters. Therefore, the application of the adsorption mathematical models in packed bed column study is vital to offer further explanation of the packed column performance. The packed column parameters indicated the major impacts in the packed bed column performance to the effective removal of the phenol and cyanide.

Acknowledgment

This study was financially supported by the MHRD. The authors are thankful to Department of Chemical Engineering and Institute Instrumentation Center of Indian Institute of Technology Roorkee, India for providing technical support and facilities.

References

- [1] M.W. Lee, J.M. Park, Biological nitrogen removal from coke plant wastewater with external carbon addition, *Water Environ. Res.* 70 (1998) 1090–1095.
- [2] I. Vázquez, J. Rodríguez, E. Marañón, L. Castrillón, Y. Fernández, Simultaneous removal of phenol, ammonium and thiocyanate from coke wastewater by aerobic biodegradation, *J. Hazard. Mater.* 137 (2006) 1773–1780.
- [3] G. Busca, S. Berardinelli, C. Resini, L. Arrighi, Technologies for the removal of phenol from fluid streams: A short review of recent developments, *J. Hazard. Mater.* 160 (2008) 265–288.
- [4] ATSDR, Agency for toxic substances and disease registry, US Department of Health and Human Services, Cyanide, 2006, pp. 25–72.
- [5] ATSDR, Agency for toxic substances and disease registry, US Department of Health and Human Services, Phenol, 2008, pp. 21–86.
- [6] G. Banerjee, Phenol- and thiocyanate-based wastewater treatment in RBC reactor, *J. Environ. Eng.* 122 (1996) 941–948.
- [7] Y.S. Jeong, J.S. Chung, Simultaneous removal of COD, thiocyanate, cyanide and nitrogen from coal process wastewater using fluidized biofilm process, *Process Biochem.* 41 (2006) 1141–1147.
- [8] Y.M. Li, G.W. Gu, J.F. Zhao, H.Q. Yu, Y.L. Qiu, Y.Z. Peng, Treatment of coke plant wastewater by biofilm systems for removal of organic compounds and nitrogen, *Chemosphere* 52 (2003) 997–1005.
- [9] M. Zhang, J.H. Tay, Y. Qian, X.S. Gu, Coke plant wastewater treatment by fixed biofilm system for COD and NH₃-N removal, *Water Res.* 32 (1998) 519–527.
- [10] W. Zhao, X. Huang, D. Lee, Enhanced treatment of coke plant wastewater using an anaerobic–anoxic–oxic membrane bioreactor system, *Sep. Purif. Technol.* 66 (2009) 279–286.
- [11] O.S. Bello, I.A. Adeogun, J.C. Ajaelu, E.O. Fehintola, Adsorption of methylene blue onto activated carbon derived from periwinkle shells: Kinetics and equilibrium studies, *Chem. Ecol.* 24(4) (2008) 285–295.
- [12] D. Ko, V. Lee, J.F. Porter, G. McKay, Improved design and optimization models for the fixed bed adsorption of acid dye and zinc ions from effluents, *J. Chem. Technol. Biotechnol.* 77(12) (2002) 1289–1295.
- [13] R. Aravindhan, J.R. Rao, B.U. Nair, Application of a chemically modified green macro alga as a biosorbent for phenol removal, *J. Environ. Manage.* 90(5) (2009) 1877–1883.
- [14] S.B. Divate, R.V. Hinge, S.R. Kadam, Removal of heavy metal (phenol) by using various adsorbents, *Int. J. Sci. Eng. Res.* 5(7) (2014) 673–678.

- [15] P. Jha, Rice-husk as an adsorbent for phenol removal, *Int. J. Sci. Nat.* 2(3) (2011) 593–596.
- [16] A.T. Mohd Din, B.H. Hameed, A.L. Ahmad, Batch adsorption of phenol onto physiochemical-activated coconut shell, *J. Hazard. Mater.* 161 (2009) 1522–1529.
- [17] N.C. Williams, F.W. Petersen, The optimisation of an impregnated carbon system to selectively recover cyanide from dilute solutions, *Miner. Eng.* 10(5) (1997) 483–490.
- [18] APHA, Standard Methods for Examination of Water and Wastewater, twentieth ed., American Public Health Association, Washington, DC, USA 1998.
- [19] R. Apiratikul, P. Pavasant, Batch and column studies of biosorption of heavy metals by *Caulerpa lentillifera*, *Bioresour. Technol.* 99 (2008) 2766–2777.
- [20] R.P. Han, Y. Wang, X. Zhao, Y.F. Wang, F.L. Xie, J.M. Cheng, M.S. Tang, Adsorption of methylene blue by phoenix tree leaf powder in a fixed-bed column: Experiments and prediction of breakthrough curves, *Desalination* 245 (2009) 284–297.
- [21] H.C. Thomas, Heterogeneous ion exchange in a flowing system, *J. Am. Chem. Soc.* 66(10) (1944) 1664–1666.
- [22] F. Rozada, M. Otero, A.I. García, A. Morán, Application in fixed bed systems of adsorbents obtained from sewage sludge and discarded tyres, *Dyes Pigm.* 72 (2007) 47–56.
- [23] E. Malkoc, Y. Nuhoglu, Removal of Ni(II) ions from aqueous solutions using waste of tea factory: Adsorption on a fixed-bed column, *J. Hazard. Mater.* 135 (2006) 328–336.
- [24] E. Guibal, R. Lorenzelli, T. Vincent, P. Le Cloirec, Application of silica gel to metal ion sorption: Static and dynamic removal of uranyl ions, *Environ. Technol.* 16 (1995) 101–114.
- [25] A. Wolborska, Adsorption on activated carbon of p-nitrophenol from aqueous solution, *Water Res.* 23 (1989) 85–91.
- [26] D. Park, Y.S. Yun, J.M. Park, The past, present and future trends of biosorption, *Biotechnol. Bioprocess Eng.* 15 (2010) 86–102.
- [27] Y.H. Yoon, J.H. Nelson, Application of gas adsorption kinetics I. A theoretical model for respirator cartridge service life, *Am. Ind. Hyg. Assoc. J.* 45(8) (1984) 509–516.
- [28] S.S. Baral, N. Das, T.S. Ramulu, S.K. Sahoo, S.N. Das, G.R. Chaudhury, Removal of Cr(VI) by thermally activated weed *Salvinia cucullata* in a fixed-bed column, *J. Hazard. Mater.* 161 (2009) 1427–1435.
- [29] M. Jung, K. Ahn, Y. Lee, K. Kim, J. Rhee, J.T. Park, K. Paeng, Adsorption characteristics of phenol and chlorophenols on granular activated carbons (GAC), *Microchem. J.* 70 (2001) 123–131.
- [30] V.C. Taty-Costodes, H.H. Fauduet, C.C. Porte, Y.S. Ho, Removal of lead(II) ions from synthetic and real effluents using immobilized *Pinus sylvestris* sawdust: Adsorption on a fixed-bed column, *J. Hazard. Mater.* 123 (2005) 135–144.
- [31] B. Volesky, I. Prasetyo, Cadmium removal in a biosorption column, *Biotechnol. Bioeng.* 43 (1994) 1010–1015.
- [32] K. Vijayaraghavan, J. Jegan, K. Palanivelu, M. Velan, Removal of nickel(II) ions from aqueous solution using crab shell particles in a packed bed up-flow column, *J. Hazard. Mater.* 113 (2004) 223–230.
- [33] X. Xu, B. Gao, X. Tan, X. Zhang, Q. Yue, Y. Wang, Q. Li, Nitrate adsorption by stratified wheat straw resin in lab-scale columns, *Chem. Eng. J.* 226 (2013) 1–6.
- [34] J.R. Rao, T. Viraraghavan, Biosorption of phenol from an aqueous solution by *Aspergillus niger* biomass, *Bioresour. Technol.* 85 (2002) 165–171.
- [35] A. Mittal, J. Mittal, L. Kurup, Adsorption isotherms, kinetics and column operations for the removal of hazardous dye, Tartrazine from aqueous solutions using waste materials—Bottom ash and de-oiled soya, as adsorbents, *J. Hazard. Mater.* 136 (2006) 567–578.
- [36] I.A.W. Tan, A.L. Ahmad, B.H. Hameed, Adsorption of basic dye using activated carbon prepared from oil palm shell: Batch and fixed bed studies, *Desalination* 225 (2008) 13–28.
- [37] A. Olgun, N. Atar, S. Wang, Batch and column studies of phosphate and nitrate adsorption on waste solids containing boron impurity, *Chem. Eng. J.* 222 (2013) 108–119.
- [38] S.R. Pilli, V.V. Goud, K. Mohanty, Biosorption of Cr(VI) on immobilized *Hydrilla verticillata* in a continuous up-flow packed bed: prediction of kinetic parameters and breakthrough curves, *Desalin. Water Treat.* 50(1–3) (2012) 115–124.
- [39] Z. Aksu, F. Gönen, Biosorption of phenol by immobilized activated sludge in a continuous packed bed: Prediction of breakthrough curves, *Process Biochem.* 39 (2004) 599–613.
- [40] Z.Z. Chowdhury, S.M. Zain, A.K. Rashid, R.F. Rafique, K. Khalid, Breakthrough curve analysis for column dynamics sorption of Mn(II) Ions from wastewater by using *Mangostana garcinia* peel-based granular-activated carbon, *J. Chem.* (2013) 1–8.
- [41] E.D. Woumfo, J.M. Siéwé, D. Njopwouo, A fixed-bed column for phosphate removal from aqueous solutions using an andosol-bagasse mixture, *J. Environ. Manage.* 151 (2015) 450–460.
- [42] G.S. Bohart, E.Q. Adams, Some aspects of the behavior of charcoal with respect to chlorine, *J. Am. Chem. Soc.* 42 (1920) 523–544.
- [43] K.S. Bharrathi, N. Badabhagn, P.V. Nidheesh, Breakthrough Data analysis of adsorption of Cd (II) on coir pith column, *Elec. J. Environ. Agric. F. Chem.* 10(8) (2011) 2638–2658.
- [44] K.M. Sreenivas, M.B. Inarkar, S.V. Gokhale, S.S. Lele, Re-utilization of ash gourd (*Benincasa hispida*) peel waste for chromium (VI) biosorption: Equilibrium and column studies, *J. Environ. Chem. Eng.* 2 (2014) 455–462.
- [45] A.D. Dorado, X. Gamisans, C. Valderrama, M. Sole, C. Lao, Cr(III) removal from aqueous solution: A straight forward model approaching of the adsorption in a fixed-bed column, *J. Environ. Sci. Health A: Tox. Hazard. Subst. Environ. Eng.* 49(2) (2014) 179–186.
- [46] V.K. Gupta, A. Rastogi, Sorption and desorption studies of chromium(VI) from nonviable cyanobacterium *Nostoc muscorum* biomass, *J. Hazard. Mater.* 154 (2008) 347–354.
- [47] G.S. Simate, S. Ndlovu, The removal of heavy metals in a packed bed column using immobilized cassava peel waste biomass, *J. Ind. Eng. Chem.* 21 (2015) 635–643.